An Overview of OFDM-Based Visible Light Communication Systems From the Perspective of Energy Efficiency Versus Spectral Efficiency

YAQI SUN[1], FANG YANG[1,2], (Senior Member, IEEE),
AND LING CHENG[3], (Senior Member, IEEE)

[1]Department of Electronic Engineering, Beijing National Research Center for Information Science and Technology, Tsinghua University, Beijing 100084, China
[2]Key Laboratory of Digital TV System of Guangdong Province and Shenzhen City, Research Institute of Tsinghua University in Shenzhen, Shenzhen 518057, China
[3]School of Electrical and Information Engineering, University of the Witwatersrand, Johannesburg 2000, South Africa

Corresponding author: Fang Yang (fangyang@tsinghua.edu.cn)

ABSTRACT In this paper, the energy efficiency and the spectral efficiency for orthogonal frequency division multiplexing (OFDM)-based visible light communication schemes are studied, which is crucial for practical application with limited energy resources. The conventional schemes, including asymmetrically clipped optical OFDM (ACO-OFDM), pulse-amplitude-modulated discrete multitone, and direct current biased optical OFDM, are compared in terms of energy efficiency and spectral efficiency relationship. The influence of power allocation for asymmetrically clipped dc biased optical OFDM and hybrid ACO-OFDM is also investigated. The energy efficiency and spectral efficiency of layered ACO-OFDM with a variable layer number are calculated and their relationship is also formulated. These conventional and hybrid modulation schemes are analyzed and compared through computer simulations, which should be considered in practice according to the requirements of illumination and transmission.

I. INTRODUCTION

The data traffic of conventional radio frequency communication is growing exponentially [1]. Recently, visible light communication (VLC) has drawn increasing attention as a potential complementary technology owing to its unlicensed spectrum resource [2], [3]. Single subcarrier schemes, such as on-off keying (OOK) and pulse position modulation (PPM) may suffer from inter-symbol interference (ISI) for high-data-rate transmission. Thus, orthogonal frequency division multiplexing (OFDM) is considered as a promising strategy to transmit high data rates [4]. The data transmission in VLC is usually realized by intensity modulation and direct detection (IM/DD) [5], where the electrical signal has to be transformed into a real-valued and nonnegative waveform for driving light emitting diodes (LEDs). The conventional OFDM for radio frequency (RF) communication, which generates complex and bipolar signals by inverse fast Fourier transform (IFFT), cannot be directly utilized for VLC. Therefore, appropriate conversions have to be developed for optical OFDM systems. The real-valued output of the IFFT is realized by imposing a Hermitian symmetry constraint to the frequency-domain signal. Apart from that, several schemes have been proposed to guarantee the unipolarity such as asymmetrically clipped optical OFDM (ACO-OFDM) [6], pulse-amplitude-modulated discrete multitone (PAM-DMT) [7], and direct current biased optical OFDM (DCO-OFDM) [8]. ACO-OFDM and PAM-DMT only utilize the odd subcarriers and the imaginary part of subcarriers, respectively, resulting in loss of spectral efficiency. Some strategies can help ameliorate the situation. In literature [9], asymmetrically clipped DC biased optical OFDM (ADO-OFDM) is introduced, which is a combination of ACO-OFDM and DCO-OFDM. A hybrid ACO-OFDM (HACO-OFDM) is also described

Y. Sun *et al.*: Overview of OFDM-Based VLC Systems From the Perspective of Energy Efficiency Versus Spectral Efficiency

IEEE *Access*

by integrating ACO-OFDM and PAM-DMT [10]. Recently, a spectrally efficient strategy called layered ACO-OFDM (LACO-OFDM) or enhanced ACO-OFDM (eACO-OFDM) is proposed, which combines multilayer signals for simultaneous transmission [11]–[13].

With the enormous increase of communication devices, the energy efficiency, which is defined as the transmitted data rate per power consumption, is widely considered in green communication [14]. Spectral efficiency, i.e., the transmitted data rate per bandwidth, is a conventional metric for communication system, which can be improved by amplifying the power. However, the energy efficiency may suffer a decrease with the increase of the spectral efficiency. It is a challenge to guarantee the quality of service (QoS) with affordable energy for the application of the Internet of things (IoT). Therefore, a tradeoff is supposed to be made between the energy efficiency and the spectral efficiency. The tradeoff between energy efficiency and spectral efficiency has been investigated for radio frequency communication. In literature [15], the relationship between the energy and spectral efficiency is proved to be quasiconcave for downlink OFDM access (OFDMA) network. A multi-objective optimization approach is proposed for the tradeoff problem in [16]. For DCO-OFDM-based VLC systems, the relationship of energy efficiency and spectral efficiency is investigated in [17], where the energy efficiency is defined as the data rate per power consumed by LED.

In VLC, the performances of different modulation schemes are affected by some parameters. For DCO-OFDM, a low DC bias will affect the channel capacity due to the remaining negative signals, while a high DC bias will make the signal higher than the upper bound of the dynamic range. Therefore, it is important to explore the influence of different DC biases on the energy-spectral efficiency. For HACO-OFDM and ADO-OFDM, different power distributions result in different performances, which should be taken into consideration. As for LACO-OFDM, more layers lead to higher spectral efficiency since the number of modulated subcarriers increases, which however causes larger power cost.

In this paper, the OFDM-based modulation schemes are comprehensively analyzed from the perspective of their energy and spectral efficiencies, which is crucial for practical application with limited energy resources in VLC. To optimize the consumed energy per bit, the energy efficiency versus spectral efficiency curves for various modulation schemes are mathematically formulated and compared to investigate the adaptive modulation according to different transmission and illumination requirements. The influence factors, such as the DC bias, the power allocation and layer number, are varied to decide the optimal parameter setup for each modulation scheme under various application environments.

The rest of this paper is organized as follows. In Section II, the models of the OFDM-based systems and the optical channel are introduced. The energy efficiency and spectral efficiency for different OFDM-based VLC modulation schemes are investigated in Section III. Simulation results

are presented in Section IV, while this paper concludes in Section V.

II. SYSTEM MODEL
A. MODULATION SCHEMES
Fig. 1 illustrates which of the first 16 out of 64 subcarriers are utilized for different modulations, including ACO-OFDM, PAM-DMT, DCO-OFDM, ADO-OFDM, HACO-OFDM, and LACO-OFDM. Without loss of generality, the 3-Layer LACO-OFDM is presented as an example of LACO-OFDM.

1) ACO-OFDM
In ACO-OFDM, the data are only carried by odd subcarriers. Considering the Hermitian symmetry, the N-point frequency-domain signal can be denoted as $X = [0, X_1, 0, X_3, \ldots, X_{N/2-1}, 0, X^*_{N/2-1}, \ldots, X^*_3, 0, X^*_1]$. The time-domain signal x_n has the anti-symmetric property as $x_n = -x_{n+N/2}$, $(0 \le n < N/2)$. The ACO-OFDM signal, $x_{\text{ACO},n}$, is generated by clipping the negative part as

$$x_{\text{ACO},n} = \begin{cases} x_n, & x_n \ge 0, \\ 0, & x_n < 0, \end{cases} \quad (1)$$

where the data information is not lost. The transmitted data can be demodulated correctly since the clipping noise only falls on the even subcarriers.

According to the central limit theorem, the unipolar signal obeys a clipped Gaussian distribution. σ^2_{A} refers to the variance of x_n, then the mean value and mean square value of $x_{\text{ACO},n}$ can be calculated as $E[x_{\text{ACO},n}] = \sigma_{\text{A}}/\sqrt{2\pi}$, and $E[x^2_{\text{ACO},n}] = \sigma^2_{\text{A}}/2$.
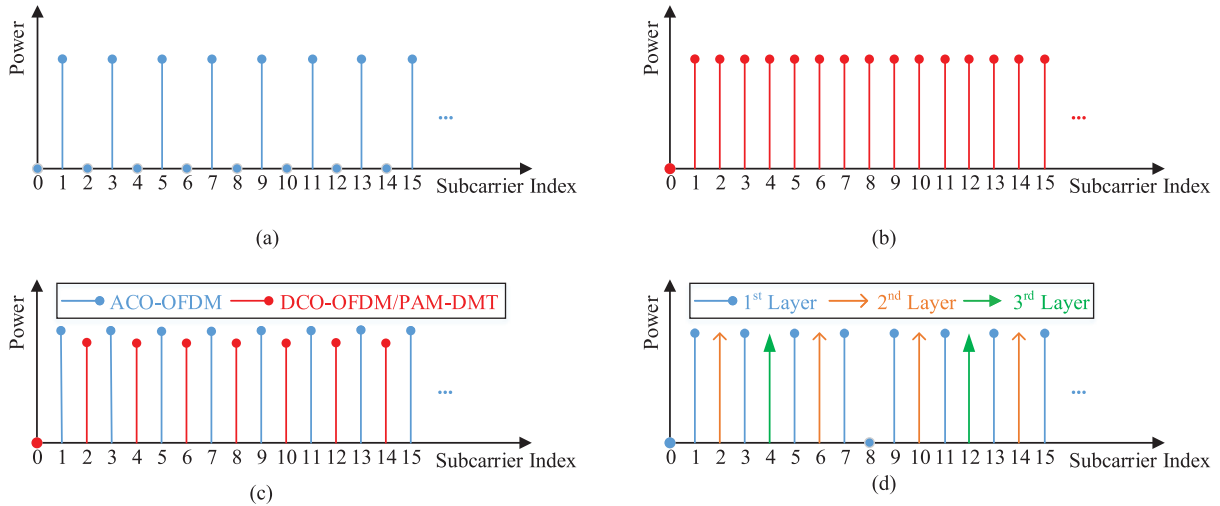
2) PAM-DMT
In PAM-DMT, real-valued signals drawn from PAM are modulated onto the imaginary part of each subcarrier except the 0-th and $N/2$-th subcarriers. The signal in the frequency domain can by represented as $Y = [0, Y_1, Y_2, \ldots, Y_{N/2-1}, 0, Y^*_{N/2-1}, \ldots, Y^*_1]$, where $Y_k = ib_k$, b_k $(k = 1, 2, \ldots, N/2 - 1)$ is the PAM signal and $i^2 = -1$. It has been proved that the time-domain signal y_n follows the symmetry as $y_n = -y_{N-n}$, $(0 \le n < N/2)$ [10]. Therefore, PAM-DMT signal $y_{\text{PAM},n}$ can also be clipped at zero, which is given by

$$y_{\text{PAM},n} = \begin{cases} y_n, & y_n \ge 0, \\ 0, & y_n < 0. \end{cases} \quad (2)$$

The clipping noise only falls on the real part of each subcarrier, leaving the transmitted data easy for demodulation [10].

Similarly to ACO-OFDM, it is easy to calculate the expectations of $y_{\text{PAM},n}$ and $y^2_{\text{PAM},n}$ as $E[y_{\text{PAM},n}] = \sigma_{\text{P}}/\sqrt{2\pi}$, and $E[y^2_{\text{PAM},n}] = \sigma^2_{\text{P}}/2$, where σ^2_{P} is the variance of y_n.

IEEE *Access*

Y. Sun *et al.*: Overview of OFDM-Based VLC Systems From the Perspective of Energy Efficiency Versus Spectral Efficiency

FIGURE 1. The modulated subcarriers for different modulation schemes. (a) ACO-OFDM. (b) PAM-DMT or DCO-OFDM. (c) ADO-OFDM or HACO-OFDM. (d) 3-Layer LACO-OFDM.

3) DCO-OFDM

In DCO-OFDM, the complex-valued frequency-domain signal is $Z = [0, Z_1, Z_2, \ldots, Z_{N/2-1}, 0, Z^*_{N/2-1}, \ldots, Z^*_1]$. A DC bias, z_b, is added to the time-domain signal, z_n, so that most of the signal is positive. The remaining negative signal will be clipped at zero, leading to a clipping noise, which depends on the DC bias.

The mean value and mean square value of $z_{\text{DCO},n}$ can be calculated as [25]

$$E\left[z_{\text{DCO},n}\right] = \sigma_D G\left(\frac{z_b}{\sigma_D}\right) + z_b\left(1 - Q\left(\frac{z_b}{\sigma_D}\right)\right), \quad (3)$$

$$E\left[z^2_{\text{DCO},n}\right] = \left(\sigma^2_D + z^2_b\right)\left(1 - Q\left(\frac{z_b}{\sigma_D}\right)\right) + z_b\sigma_D G\left(\frac{z_b}{\sigma_D}\right), \quad (4)$$

where σ^2_D is the variance of z_n. $G(\cdot)$ and $Q(\cdot)$ represent the standard Gaussian distribution and the tail probability of the standard normal distribution, respectively, which are given by

$$G(\omega) = \frac{1}{\sqrt{2\pi}}\exp\left(-\frac{\omega^2}{2}\right), \quad (5)$$

$$Q(\omega) = \frac{1}{\sqrt{2\pi}}\int_\omega^\infty \exp\left(-\frac{\lambda^2}{2}\right)d\lambda, \quad (6)$$

where λ represents the integral variable. Usually, z_b is relative to the electrical power of the signal z_n, and can be set to $z_b = \mu\sqrt{E\{z^2_n\}} = \mu\sigma_D$, where μ is a proportional constant.

4) HACO-OFDM

HACO-OFDM is a combination of ACO-OFDM and PAM-DMT, where the information is carried by the odd subcarriers and the imaginary part of the even subcarriers. The negative part is clipped individually for the two varieties of signals. Then the two signals are added together for simultaneous

transmission. The obtained time-domain HACO-OFDM signal, $s_{\text{HACO},n}$, is denoted as

$$s_{\text{HACO},n} = x_{\text{ACO},n} + y_{\text{PAM},n}. \quad (7)$$

5) ADO-OFDM

Similarly to HACO-OFDM, ADO-OFDM combines ACO-OFDM with DCO-OFDM. The ACO-OFDM signal is obtained by using the conventional method. The other stream of signal only utilized even subcarriers with a DC bias. Then, the transmitted ADO-OFDM signal, $s_{\text{ADO},n}$, is obtained by adding them together as

$$s_{\text{ADO},n} = x_{\text{ACO},n} + z_{\text{DCO},n}. \quad (8)$$

6) LACO-OFDM

The LACO-OFDM scheme consists of multiple layers of ACO-OFDM signals. For clarity, L-Layer LACO-OFDM denotes a LACO-OFDM with L layers, while l-th ACO-OFDM refers to the l-th layer in LACO-OFDM.

In the l-th ACO-OFDM, only the $2^{l-1}(2k+1)$-th ($k = 0, 1, \ldots, N/2^l - 1$) subcarriers are modulated, denoted as $X^{(l)}_{\text{ACO},k}$. For each layer, the negative part of the time-domain signal can be clipped without loss of any information, resulting in $x^{(l)}_{\text{ACO},n}$. Then the several streams of non-negative signals are superposed together and transmitted simultaneously as

$$s_{L,n} = \sum_{l=1}^L x^{(l)}_{\text{ACO},n}. \quad (9)$$

B. CHANNEL MODEL

The channel for VLC can be modeled as a linear time-invariant channel with the additive white Gaussian noise (AWGN), where the channel frequency response can be considered to be flat near DC [20]. The transmitted signal generated by different schemes, including $x_{\text{ACO},n}$, $y_{\text{PAM},n}$,

Y. Sun *et al.*: Overview of OFDM-Based VLC Systems From the Perspective of Energy Efficiency Versus Spectral Efficiency

IEEE *Access*

$z_{DCO,n}$, $s_{HACO,n}$, $s_{ADO,n}$ and $s_{L,n}$, are generalized as s_n. Then, the received signal, r_n, can be represented as

$$r_n = H_0 R s_n + v_n, \tag{10}$$

where H_0 denotes the channel DC gain, v_n is referred to as AWGN, and R is the combined coefficient including the voltage-current transfer, the LED responsivity, and the detector responsivity.
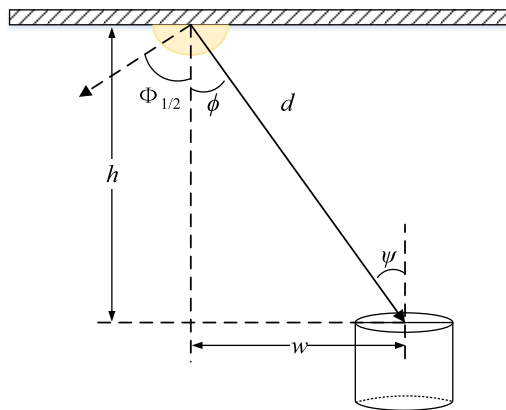

FIGURE 2. The geometry for VLC systems.

Fig. 2 demonstrates a geometry for VLC systems, which is considered in this paper, where $\Phi_{1/2}$ is the transmitter semiangle, the light radiance and incidence angles are ϕ and ψ, respectively. h and w represent the vertical and horizontal distances between the transmitter and the receiver, respectively. And $d = \sqrt{h^2 + w^2}$ is the direct distance. In line-of-sight links, the DC gain can be modeled with a generalized Lambertian radiant intensity as [21]–[23]

$$H_0 = \frac{(m+1)A}{2\pi d^2} \cos^m(\phi) T(\psi) g(\psi) \cos(\psi), \tag{11}$$

where $m = -1/\log_2(\cos(\Phi_{1/2}))$ is the Lambertian order and A denotes the detector physical area. $T(\psi)$ is the filter gain which can be set to 1 for simplification. $g(\psi)$ is the concentrator gain, which is given by

$$g(\psi) = \begin{cases} \dfrac{v^2}{\sin^2 \Psi_c}, & 0 \le \psi \le \Psi_c, \\ 0, & \psi > \Psi_c, \end{cases} \tag{12}$$

where Ψ_c refers to the field of view (FOV) of the concentrator and v is the internal refractive index. As shown in Fig. 2, the relationship between the angle and the distance can be given as

$$\cos(\psi) = \cos(\phi) = \frac{h}{\sqrt{h^2 + w^2}}. \tag{13}$$

Thus, for $0 \le \psi \le \Psi_c$, the DC gain can be derived as

$$H_0 = \frac{(m+1)Av^2}{2\pi \sin^2 \Psi_c} \frac{h^{m+1}}{\left(\sqrt{h^2 + w^2}\right)^{m+3}}. \tag{14}$$
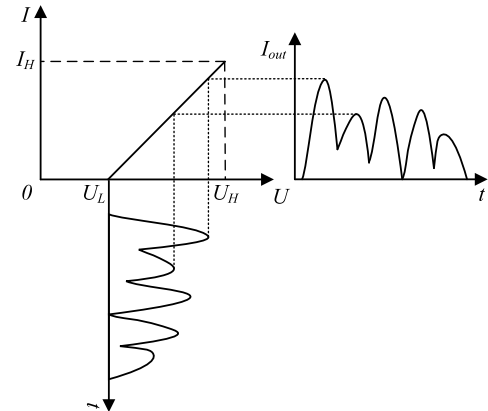

FIGURE 3. The current-voltage relationship for LED.

The turn-on voltage (TOV) of LED is the minimum threshold value for the input that can generate current. The nonlinearity of LED can be mitigated by the methods proposed in [24]. Thus the current-voltage relationship can be quasi-linear in a limited range, as shown in Fig. 3, where U_L denotes the LED TOV, U_H and I_H refer to the maximum allowable voltage and current, respectively. The reciprocal of the slope can be calculated as $\kappa = (U_H - U_L)/I_H$.

A proper DC bias has to be added to the OFDM-based VLC signal in consideration of the TOV. Since the OFDM-based VLC signal is non-negative, the DC bias is supposed to be equal to U_L. Thus, the input voltage can be given by

$$U_n = \kappa s_n + U_L. \tag{15}$$

III. SPECTRAL EFFICIENCY AND ENERGY EFFICIENCY

For VLC systems, the spectral efficiency can be defined as the channel capacity per unit of bandwidth, which is given by

$$\eta_{SE} = \frac{C}{W}, \tag{16}$$

where C and W denote the channel capacity and the whole bandwidth, respectively. The energy efficiency is defined as the ratio of the channel capacity over the mean power consumption [17], which is given by

$$\eta_{EE} = \frac{C}{P}, \tag{17}$$

where P denotes the LED power cost. It is worth mentioning that the power is also cost by the conversion of base-band electrical signals into respective OFDM/DMT signals, which, however, is too complicated to analyze. Thus, this paper only focuses on the power consumption by the LED. In this section, the spectral efficiency and energy efficiency for OFDM-based VLC modulation schemes are investigated.

A. ACO-OFDM

Since the amplitude of the clipped signal in the frequency domain is halved, the signal-to-noise ratio (SNR) for each

subcarrier is

$$\xi_{\text{ACO}} = \frac{H_0^2 R^2 \frac{1}{4} \varepsilon_A}{\sigma_n^2} = \frac{H_0^2 R^2 \varepsilon_A}{4\sigma_n^2}, \tag{18}$$

where ε_A denotes the variance of the modulated symbol X_{2k+1} ($k = 0, 1, \ldots N/4 - 1$), $\sigma_n^2 = N_0 W/N$ is the variance of the AWGN noise. Considering that only the odd subcarriers are utilized in ACO-OFDM, the relationship between ε_A and σ_A^2 can be derived as

$$\sigma_A^2 = \frac{\varepsilon_A}{2}. \tag{19}$$

The total channel capacity for ACO-OFDM can be calculated as

$$\begin{aligned} C_{\text{ACO}} &= \frac{N}{4} \frac{W}{N} \log_2 (1 + \xi_{\text{ACO}}) \\ &= \frac{W}{4} \log_2 \left(1 + \frac{H_0^2 R^2 \varepsilon_A}{4\sigma_n^2}\right) \\ &= \frac{W}{4} \log_2 \left(1 + \frac{H_0^2 R^2 \sigma_A^2}{2\sigma_n^2}\right). \end{aligned} \tag{20}$$

Thus, the spectral efficiency for ACO-OFDM is given by

$$\begin{aligned} \eta_{\text{SE,ACO}} &= \frac{C_{\text{ACO}}}{W} \\ &= \frac{1}{4} \log_2 \left(1 + \frac{H_0^2 R^2 \sigma_A^2}{2\sigma_n^2}\right). \end{aligned} \tag{21}$$

The power consumed by LED can be formulated as

$$\begin{aligned} P_{\text{ACO}} &= E[U_n I_n] \\ &= E[(\kappa x_{\text{ACO},n} + U_L) x_{\text{ACO},n}] \\ &= \kappa E[x_{\text{ACO},n}^2] + U_L E[x_{\text{ACO},n}] \\ &= \kappa \frac{\sigma_A^2}{2} + U_L \frac{\sigma_A}{\sqrt{2\pi}}. \end{aligned} \tag{22}$$

Then the energy efficiency can be derived as

$$\begin{aligned} \eta_{\text{EE,ACO}} &= \frac{C_{\text{ACO}}}{P_{\text{ACO}}} \\ &= \frac{\frac{W}{4} \log_2 \left(1 + \frac{H_0^2 R^2 \sigma_A^2}{2\sigma_n^2}\right)}{\kappa \frac{\sigma_A^2}{2} + U_L \frac{\sigma_A}{\sqrt{2\pi}}}. \end{aligned} \tag{23}$$

Based on (21) and (23), the relationship between spectral efficiency and energy efficiency for ACO-OFDM can be deduced as

$$\eta_{\text{EE,ACO}} = \frac{W \eta_{\text{SE,ACO}}}{\frac{\kappa \sigma_n^2 \left(2^{4\eta_{\text{SE,ACO}}} - 1\right)}{H_0^2 R^2} + \frac{U_L \sigma_n}{\sqrt{\pi} H_0 R} \sqrt{2^{4\eta_{\text{SE,ACO}}} - 1}}. \tag{24}$$

B. PAM-DMT

The spectral efficiency and the energy efficiency for PAM-DMT are similar to that for ACO-OFDM. The SNR for each subcarrier is

$$\xi_{\text{PAM}} = \frac{H_0^2 R^2 \frac{1}{4} \varepsilon_P}{\frac{1}{2} \sigma_n^2} = \frac{H_0^2 R^2 \varepsilon_P}{2\sigma_n^2}, \tag{25}$$

where $\varepsilon_P = E[Y_k^2]$ ($k = 1, 2, \ldots N/2 - 1$). Since the 0-th and the $N/2$-th subcarrier are set to zeros, the relationship between ε_P and σ_P^2 is given by

$$\sigma_P^2 = \frac{(N-2)\varepsilon_P}{N}. \tag{26}$$

Considering that the data is only modulated onto the imaginary part of the subcarriers, the total channel capacity for PAM-DMT is calculated as

$$\begin{aligned} C_{\text{PAM}} &= \frac{1}{2} \frac{N-2}{2} \frac{W}{N} \log_2 (1 + \xi_{\text{PAM}}) \\ &= \frac{(N-2)W}{4N} \log_2 \left(1 + \frac{H_0^2 R^2 \varepsilon_P}{2\sigma_n^2}\right) \\ &= \frac{(N-2)W}{4N} \log_2 \left(1 + \frac{N H_0^2 R^2 \sigma_P^2}{2(N-2)\sigma_n^2}\right). \end{aligned} \tag{27}$$

Then, the spectral efficiency is derived as

$$\begin{aligned} \eta_{\text{SE,PAM}} &= \frac{C_{\text{PAM}}}{W} \\ &= \frac{N-2}{4N} \log_2 \left(1 + \frac{N H_0^2 R^2 \sigma_P^2}{2(N-2)\sigma_n^2}\right). \end{aligned} \tag{28}$$

The power consumed by LED for PAM-DMT is given by

$$\begin{aligned} P_{\text{PAM}} &= \kappa E[y_{\text{PAM},n}^2] + U_L E[y_{\text{PAM},n}] \\ &= \kappa \frac{\sigma_P^2}{2} + U_L \frac{\sigma_P}{\sqrt{2\pi}}. \end{aligned} \tag{29}$$

Thus, the energy efficiency can be represented as

$$\begin{aligned} \eta_{\text{EE,PAM}} &= \frac{C_{\text{PAM}}}{P_{\text{PAM}}} \\ &= \frac{\frac{(N-2)W}{4N} \log_2 \left(1 + \frac{N H_0^2 R^2 \sigma_P^2}{2(N-2)\sigma_n^2}\right)}{\kappa \frac{\sigma_P^2}{2} + U_L \frac{\sigma_P}{\sqrt{2\pi}}}. \end{aligned} \tag{30}$$

The energy efficiency can be derived as a function of the spectral efficiency as

$$\eta_{\text{EE,PAM}} = \frac{W \eta_{\text{SE,PAM}}}{\frac{\alpha_P \kappa \sigma_n^2 \left(2^{\frac{4\eta_{\text{SE,PAM}}}{\alpha_P}} - 1\right)}{H_0^2 R^2} + \sqrt{\frac{\alpha_P}{\pi}} \frac{U_L \sigma_n}{H_0 R} \sqrt{2^{\frac{4\eta_{\text{SE,PAM}}}{\alpha_P}} - 1}}, \tag{31}$$

where $\alpha_P = (N-2)/N$.

Y. Sun *et al.*: Overview of OFDM-Based VLC Systems From the Perspective of Energy Efficiency Versus Spectral Efficiency

IEEE *Access*

C. DCO-OFDM

For DCO-OFDM, the remaining negative signal after adding the DC bias will be clipped at zero. Thus, the transmitted DCO-OFDM signal can be modeled as $z_{\text{DCO},n} = z_{\text{clip},n} + z_b$, where $z_{\text{clip},n}$ is the signal clipped at a level of $-z_b$, i.e.,

$$z_{\text{clip},n} = \begin{cases} z_n, & z_n > -z_b, \\ -z_b, & z_n \leq -z_b. \end{cases} \tag{32}$$

Based on Bussgang theorem, $z_{\text{clip},n}$ can be modeled as

$$z_{\text{clip},n} = cz_n + n_{\text{DCO},n}, \tag{33}$$

where $n_{\text{DCO},n}$ is the clipping distortion and c is a constant, which can be calculated as [25]

$$c = 1 - Q\left(\frac{z_b}{\sigma_{\text{D}}}\right), \tag{34}$$

where $\sigma_{\text{D}}^2 = E[z_n^2]$.

Based on (3) and (4), the mean value and mean square value of $z_{\text{clip},n}$ can be calculated as

$$E\left[z_{\text{clip},n}\right] = E\left[z_{\text{DCO},n}\right] - z_b$$
$$= \sigma_{\text{D}} G\left(\frac{z_b}{\sigma_{\text{D}}}\right) - z_b Q\left(\frac{z_b}{\sigma_{\text{D}}}\right), \tag{35}$$

$$E\left[z_{\text{clip},n}^2\right] = E\left[\left(z_{\text{DCO},n} - z_b\right)^2\right]$$
$$= E\left[z_{\text{DCO},n}^2\right] + z_b^2 - 2z_b E\left[z_{\text{DCO},n}\right]$$
$$= \sigma_{\text{D}}^2 + \left(z_b^2 - \sigma_{\text{D}}^2\right) Q\left(\frac{z_b}{\sigma_{\text{D}}}\right) - z_b \sigma_{\text{D}} G\left(\frac{z_b}{\sigma_{\text{D}}}\right), \tag{36}$$

Then, the variance of the clipping distortion can be calculated as [25]

$$\sigma_{\text{clip}}^2 = E\left[z_{\text{clip},n}^2\right] - c^2 \sigma_{\text{D}}^2 - E\left[z_{\text{clip},n}\right]^2$$
$$= \sigma_{\text{D}}^2 + \left(z_b^2 - \sigma_{\text{D}}^2\right) Q\left(\frac{z_b}{\sigma_{\text{D}}}\right)$$
$$- z_b \sigma_{\text{D}} G\left(\frac{z_b}{\sigma_{\text{D}}}\right) - \sigma_{\text{D}}^2 Q\left(-\frac{z_b}{\sigma_{\text{D}}}\right)^2$$
$$- \left(\sigma_{\text{D}} G\left(\frac{z_b}{\sigma_{\text{D}}}\right) - z_b Q\left(\frac{z_b}{\sigma_{\text{D}}}\right)\right)^2. \tag{37}$$

By taking clipping distortion into consideration, the signal-to-noise-plus-distortion (SNDR) for each subcarrier can be calculated as

$$\xi_{\text{DCO}} = \frac{H_0^2 R^2 c^2 \sigma_{\text{D}}^2}{H_0^2 R^2 \sigma_{\text{clip}}^2 + \sigma_{\text{n}}^2}. \tag{38}$$

And the total channel capacity is given by

$$C_{\text{DCO}} = \frac{N-2}{2} \frac{W}{N} \log_2\left(1 + \xi_{\text{DCO}}\right)$$
$$= \frac{(N-2)W}{2N} \log_2\left(1 + \frac{H_0^2 R^2 c^2 \sigma_{\text{D}}^2}{H_0^2 R^2 \sigma_{\text{clip}}^2 + \sigma_{\text{n}}^2}\right). \tag{39}$$

The power cost by LED is calculated as

$$P_{\text{DCO}} = \kappa E\left[z_{\text{DCO},n}^2\right] + U_L E\left[z_{\text{DCO},n}\right]$$
$$= \kappa \left[\left(\sigma_{\text{D}}^2 + z_b^2\right)\left(1 - Q\left(\frac{z_b}{\sigma_{\text{D}}}\right)\right) + z_b \sigma_{\text{D}} G\left(\frac{z_b}{\sigma_{\text{D}}}\right)\right]$$
$$+ U_L \left[\sigma_{\text{D}} G\left(\frac{z_b}{\sigma_{\text{D}}}\right) + z_b \left(1 - Q\left(\frac{z_b}{\sigma_{\text{D}}}\right)\right)\right]. \tag{40}$$

Thus, the spectral efficiency and energy efficiency for DCO-OFDM can be formulated as

$$\eta_{\text{SE,DCO}} = \frac{C_{\text{DCO}}}{W}$$
$$= \frac{N-2}{2N} \log_2\left(1 + \frac{H_0^2 R^2 c^2 \sigma_{\text{D}}^2}{H_0^2 R^2 \sigma_{\text{clip}}^2 + \sigma_{\text{n}}^2}\right), \tag{41}$$

$$\eta_{\text{EE,DCO}} = \frac{C_{\text{DCO}}}{P_{\text{DCO}}}$$
$$= \frac{\frac{(N-2)W}{2N} \log_2(1 + \frac{H_0^2 R^2 c^2 \sigma_{\text{D}}^2}{H_0^2 R^2 \sigma_{\text{clip}}^2 + \sigma_{\text{n}}^2})}{\kappa E\left[z_{\text{DCO},n}^2\right] + U_L E\left[z_{\text{DCO},n}\right]}. \tag{42}$$

D. HACO-OFDM

In HACO-OFDM systems, the ACO-OFDM signal occupies odd subcarriers, whereas the PAM-DMT occupies $(N/2 - 2)$ subcarriers. Thus, σ_{A}^2 and σ_{P}^2 can be calculated as

$$\sigma_{\text{A}}^2 = \frac{\varepsilon_{\text{A}}}{2}, \tag{43}$$

$$\sigma_{\text{P}}^2 = \frac{(N-4)\varepsilon_{\text{P}}}{2N}. \tag{44}$$

Thus, the channel capacity for HACO-OFDM can be formulated as

$$C_{\text{HACO}}$$
$$= \frac{W}{4} \log_2\left(1 + \xi_{\text{ACO}}\right) + \frac{(N-4)W}{8N} \log_2\left(1 + \xi_{\text{PAM}}\right)$$
$$= \frac{W}{4} \log_2\left(1 + \frac{H_0^2 R^2 \varepsilon_{\text{A}}}{4\sigma_{\text{n}}^2}\right)$$
$$+ \frac{(N-4)W}{8N} \log_2\left(1 + \frac{H_0^2 R^2 \varepsilon_{\text{P}}}{2\sigma_{\text{n}}^2}\right)$$
$$= \frac{W}{4} \log_2\left(1 + \frac{H_0^2 R^2 \sigma_{\text{A}}^2}{2\sigma_{\text{n}}^2}\right)$$
$$+ \frac{(N-4)W}{8N} \log_2\left(1 + \frac{NH_0^2 R^2 \sigma_{\text{P}}^2}{(N-4)\sigma_{\text{n}}^2}\right). \tag{45}$$

The LED power consumption is given by

$$P_{\text{HACO}}$$
$$= E\left[\left(\kappa\left(x_{\text{ACO},n} + y_{\text{PAM},n}\right) + U_L\right)\left(x_{\text{ACO},n} + y_{\text{PAM},n}\right)\right]$$
$$= \kappa E\left[x_{\text{ACO},n}^2\right] + \kappa E\left[y_{\text{PAM},n}^2\right] + 2\kappa E\left[x_{\text{ACO},n}\right] E\left[y_{\text{PAM},n}\right]$$
$$+ U_L E\left[x_{\text{ACO},n}\right] + U_L E\left[y_{\text{PAM},n}\right]$$
$$= \kappa\left(\frac{\sigma_{\text{A}}^2}{2} + \frac{\sigma_{\text{P}}^2}{2} + \frac{\sigma_{\text{A}}\sigma_{\text{P}}}{\pi}\right) + U_L \frac{\sigma_{\text{A}} + \sigma_{\text{P}}}{\sqrt{2\pi}}. \tag{46}$$

Then, the spectral efficiency and energy efficiency can be derived according to (45) and (46).

IEEE *Access*

Y. Sun *et al.*: Overview of OFDM-Based VLC Systems From the Perspective of Energy Efficiency Versus Spectral Efficiency

E. ADO-OFDM

The odd subcarriers and even subcarriers (except 0-th and $N/2$-th subcarriers) are utilized for ACO-OFDM and DCO-OFDM in ADO-OFDM systems. The channel capacity and the power cost by LED can be calculated as

$$
\begin{aligned}
&C_{\text{ADO}}\\
&= \frac{W}{4}\log_2\left(1+\xi_{\text{ACO}}\right) + \frac{(N-4)W}{4N}\log_2\left(1+\xi_{\text{DCO}}\right)\\
&= \frac{W}{4}\log_2\left(1+\frac{H_0^2 R^2 \sigma_A^2}{2\sigma_n^2}\right)\\
&\quad + \frac{(N-4)W}{4N}\log_2\left(1+\frac{H_0^2 R^2 c^2 \sigma_D^2}{H_0^2 R^2 \sigma_{\text{clip}}^2 + \sigma_n^2}\right),
\end{aligned} \tag{47}
$$

$$
\begin{aligned}
&P_{\text{ADO}}\\
&= E\left[\left(\kappa\left(x_{\text{ACO},n}+z_{\text{DCO},n}\right)+U_L\right)\left(x_{\text{ACO},n}+z_{\text{DCO},n}\right)\right]\\
&= \kappa E\left[x_{\text{ACO},n}^2\right] + \kappa E\left[z_{\text{DCO},n}^2\right] + 2\kappa E\left[x_{\text{ACO},n}\right]E\left[z_{\text{DCO},n}\right]\\
&\quad + U_L E\left[x_{\text{ACO},n}\right] + U_L E\left[z_{\text{DCO},n}\right]\\
&= \kappa\left[\left(\sigma_D^2+z_b^2\right)\left(1-Q\left(\frac{z_b}{\sigma_D}\right)\right)+z_b\sigma_D G\left(\frac{z_b}{\sigma_D}\right)\right]\\
&\quad + \left(\frac{2\kappa\sigma_A}{\sqrt{2\pi}}+U_L\right)\left[\sigma_D G\left(\frac{z_b}{\sigma_D}\right)+z_b\left(1-Q\left(\frac{z_b}{\sigma_D}\right)\right)\right]\\
&\quad + \kappa\frac{\sigma_A^2}{2} + U_L\frac{\sigma_A}{\sqrt{2\pi}}.
\end{aligned} \tag{48}
$$

Based on (47) and (48), $\eta_{\text{SE,ADO}}$ and $\eta_{\text{SE,ADO}}$ are calculable.

F. LACO-OFDM

For L-Layer LACO-OFDM, assuming that the power is equally distributed to each subcarrier [26], the variance of the modulated symbol $X_{\text{ACO},k}^{(l)}$ can be normalized as ε_L for each layer. Since only $N/2^l$ subcarriers are modulated for the l-th layer, according to the Parseval's theorem, the relationship between σ_l and ε_L can be derived as

$$
\sigma_l^2 = \frac{\varepsilon_L}{2^l}. \tag{49}
$$

Then the signal-to-noise ratio (SNR) of each modulated subcarrier is given by

$$
\xi_L = \frac{H_0^2 R^2 \varepsilon_L}{4\sigma_n^2}, \tag{50}
$$

where $\sigma_n^2 = N_0 W/N$ is the variance of the AWGN noise. N_0 is the noise power spectral density and W denotes the whole bandwidth. Then the total channel capacity of L-Layer LACO-OFDM can be calculated as

$$
\begin{aligned}
C_{\text{LACO}} &= \sum_{l=1}^{L}\frac{W}{2^{l+1}}\log_2\left(1+\frac{H_0^2 R^2 \varepsilon_L}{4\sigma_n^2}\right)\\
&= \frac{(2^L-1)W}{2^{L+1}}\log_2\left(1+\frac{H_0^2 R^2 \varepsilon_L}{4\sigma_n^2}\right)\\
&= \alpha_L W\log_2\left(1+\frac{H_0^2 R^2 \varepsilon_L}{4\sigma_n^2}\right),
\end{aligned} \tag{51}
$$

where

$$
\alpha_L = \frac{(2^L-1)}{2^{L+1}}.
$$

The spectral efficiency is given by

$$
\eta_{\text{SE,LACO}} = \frac{C_{\text{LACO}}}{W} = \alpha_L\log_2(1+\frac{H_0^2 R^2 \varepsilon_L}{4\sigma_n^2}). \tag{52}
$$

For L-Layer LACO-OFDM systems, P_{LACO} can be calculated as

$$
P_{\text{LACO}} = \kappa E\left[(x_{L-\text{LACO}})^2\right] + U_L E\left[x_{L-\text{LACO}}\right]. \tag{53}
$$

The expectation of $s_{L,n}$ can be derived as

$$
\begin{aligned}
E\left[s_{L,n}\right] &= E\left[\sum_{l=1}^{L}x_{\text{ACO}}^{(l)}\right] = \sum_{l=1}^{L}E\left[x_{\text{ACO}}^{(l)}\right]\\
&= \frac{\sum_{l=1}^{L}\sigma_l}{\sqrt{2\pi}} = \frac{\sum_{l=1}^{L}\frac{\sqrt{\varepsilon_L}}{2^{l/2}}}{\sqrt{2\pi}}\\
&= \frac{1-\frac{1}{2^{L/2}}}{\sqrt{2}-1}\frac{\sqrt{\varepsilon_L}}{\sqrt{2\pi}} = \gamma_L\sqrt{\varepsilon_L},
\end{aligned} \tag{54}
$$

where

$$
\gamma_L = \frac{1-\frac{1}{2^{L/2}}}{\sqrt{2}-1}\frac{1}{\sqrt{2\pi}}.
$$

Considering that the signals from different layers are independent, the mean square value of $s_{L,n}$ can be formulated as

$$
\begin{aligned}
&E\left[\left(s_{L,n}\right)^2\right]\\
&= E\left[\left(\sum_{l=1}^{L}x_{\text{ACO}}^{(l)}\right)^2\right]\\
&= \sum_{l=1}^{L}E\left[\left(x_{\text{ACO}}^{(l)}\right)^2\right] + \sum_{i=1}^{L}\sum_{j=1,j\neq i}^{L}E\left[x_{\text{ACO}}^{(i)}x_{\text{ACO}}^{(j)}\right]\\
&= \sum_{l=1}^{L}E\left[\left(x_{\text{ACO}}^{(l)}\right)^2\right] + \sum_{i=1}^{L}\sum_{j=1,j\neq i}^{L}E\left[x_{\text{ACO}}^{(i)}\right]E\left[x_{\text{ACO}}^{(j)}\right].
\end{aligned} \tag{55}
$$

The first term in (55) can be simplified as

$$
\sum_{l=1}^{L}E\left[\left(x_{\text{ACO}}^{(l)}\right)^2\right] = \sum_{l=1}^{L}\frac{\sigma_l^2}{2} = \sum_{l=1}^{L}\frac{\frac{\varepsilon_L}{2^l}}{2} = \frac{2^L-1}{2^{L+1}}\varepsilon_L. \tag{56}
$$

The simplification of the second term in (55) can be given by

$$
\begin{aligned}
&\sum_{i=1}^{L}\sum_{j=1,j\neq i}^{L}E\left[x_{\text{ACO}}^{(i)}\right]E\left[x_{\text{ACO}}^{(j)}\right]\\
&= \sum_{i=1}^{L}\sum_{j=1,j\neq i}^{L}\frac{\sigma_i\sigma_j}{2\pi}\\
&= \frac{\varepsilon_L}{2\pi}\left(\sum_{i=1}^{L}\sum_{j=1,j\neq i}^{L}\frac{1}{2^{i/2}}\frac{1}{2^{j/2}}\right)
\end{aligned}
$$

Y. Sun *et al.*: Overview of OFDM-Based VLC Systems From the Perspective of Energy Efficiency Versus Spectral Efficiency

IEEE *Access*

$$= \frac{\varepsilon_L}{2\pi} \left(\sum_{i=1}^{L} \sum_{j=1}^{L} \frac{1}{2^{i/2}} \frac{1}{2^{j/2}} - \sum_{i=1}^{L} \frac{1}{2^{i/2}} \frac{1}{2^{i/2}} \right)$$

$$= \frac{\varepsilon_L}{2\pi} \left(\sum_{i=1}^{L} \left(\frac{1}{2^{i/2}} \sum_{j=1}^{L} \frac{1}{2^{j/2}} \right) - \sum_{i=1}^{L} \frac{1}{2^i} \right)$$

$$= \frac{\varepsilon_L}{2\pi} \left(\left(\frac{1 - \frac{1}{2^{L/2}}}{\sqrt{2} - 1} \right)^2 - \left(1 - \frac{1}{2^L} \right) \right)$$

$$= \left(1 + \sqrt{2} - \frac{3 + 2\sqrt{2}}{2^{L/2}} + \frac{2 + \sqrt{2}}{2^L} \right) \frac{\varepsilon_L}{\pi}. \quad (57)$$

Therefore, equation (55) can be simplified based on (56) and (57), which is given by

$$E\left[(s_{L,n})^2 \right] = \beta_L \varepsilon_L, \quad (58)$$

where

$$\beta_L = \frac{2^L - 1}{2^{L+1}} + \left(1 + \sqrt{2} - \frac{3 + 2\sqrt{2}}{2^{L/2}} + \frac{2 + \sqrt{2}}{2^L} \right) \frac{1}{\pi}.$$

Thus the power consumed by LED in (53) can be derived as

$$P_{\text{LACO}} = \beta_L \kappa \varepsilon_L + \gamma_L U_L \sqrt{\varepsilon_L}. \quad (59)$$

Then, the energy efficiency is calculated by

$$\eta_{\text{EE,LACO}} = \frac{\alpha_L W \log_2 \left(1 + \frac{H_0^2 R^2 \varepsilon_L}{4\sigma_n^2} \right)}{\beta_L \kappa \varepsilon_L + \gamma_L U_L \sqrt{\varepsilon_L}}. \quad (60)$$

According to (52), ε_L can be formulated as a function of $\eta_{\text{SE,LACO}}$, which is given by

$$\varepsilon_L = \frac{4\sigma_n^2 (2^{\eta_{\text{SE,LACO}}/\alpha_L} - 1)}{H_0^2 R^2}. \quad (61)$$

Thus, the relationship between energy efficiency and spectral efficiency can be deduced as

$$\eta_{\text{EE,LACO}} = \frac{W\eta_{\text{SE,LACO}}}{\frac{4\beta_L\kappa\sigma_n^2(2^{\eta_{\text{SE}}/\alpha_L}-1)}{H_0^2 R^2} + \frac{2\gamma_L U_L \sigma_n}{H_0 R}\sqrt{2^{\eta_{\text{SE}}/\alpha_L}-1}}. \quad (62)$$

IV. SIMULATION RESULTS

In this section, simulation results of the energy efficiency and spectral efficiency relationship are demonstrated. The simulation parameters are listed in Table 1. For fair comparison, the largest acceptable clipping ratio, which is the proportion of the signal that is higher than I_H, is set to 1%.

Fig. 4 demonstrates the spectral efficiency versus energy efficiency for the conventional ACO-OFDM, PAM-DMT, and DCO-OFDM. In DCO-OFDM, the parameter for the DC bias, μ, ranges from 1 to 4. Since no extra DC bias is added to the ACO-OFDM and PAM-DMT signals, it can be seen that these two clipping-based strategies can achieve higher energy efficiency than DCO-OFDM when η_{SE} is low. However, approximately half of the spectrum resources are

TABLE 1. Simulation parameters.

| Parameter	Value
Bandwidth, W	20 MHz
Number of subcarriers, N	64
Turn-on voltage, U_L	2.75 V
Maximum voltage, U_H	3.4 V
Maximum current, I_H	0.7 A
Transfer coefficient, R	0.5
Detector area, A	1 cm^2
Transmitter semiangle, $\Phi_{1/2}$	60°
Filter gain, $T_s(\psi)$	1
Concentrator FOV, Ψ_c	90°
Internal refractive index, ν	1.5
Noise power spectral density, N_0	1×10^{-21} A^2/Hz
Vertical distance, h	3 m
Horizontal distance, w	3 m
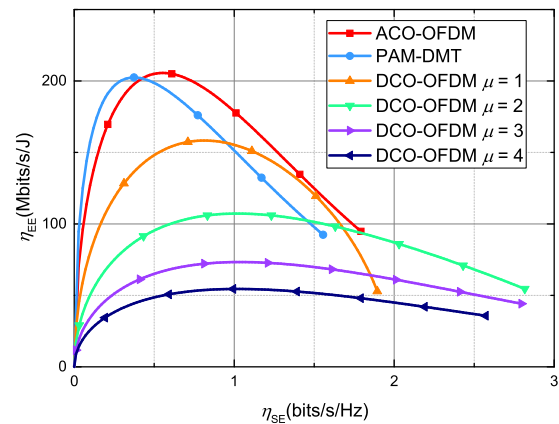
FIGURE 4. Spectral efficiency versus energy efficiency for ACO-OFDM, PAM-DMT, and DCO-OFDM.

wasted in ACO-OFDM and PAM-DMT, which leads to a limited achievable spectral efficiency in consideration of the constrained clipping ratio. The DCO-OFDM utilizes all subcarriers except 0-th and $N/2$-th subcarriers, thus the spectral efficiency can exceed 2 bits/s/Hz, as shown in Fig. 4. In DCO-OFDM, a higher DC bias results in a lower energy efficiency. Besides, the reachable η_{SE} is restricted for both small and large DC biases due to the clipping noise caused by the negative signal and the signal which is higher than I_H. According to the simulation results, the DCO-OFDM with $\mu = 2$ is relatively satisfactory.

The simulated η_{EE} and η_{SE} for HACO-OFDM with different power allocations are presented in Fig. 5. As ACO-OFDM and PAM-DMT have similar performances, the four curves are pretty close. For a low spectral efficiency, the energy efficiency increases if ACO-OFDM occupies more power. However, the largest achievable spectral efficiency decreases with the rising proportion of ACO-OFDM. All things considered, $\varepsilon_A = 4\varepsilon_P$ would be a superior choice, which has a high energy efficiency and a wide spectral efficiency range.
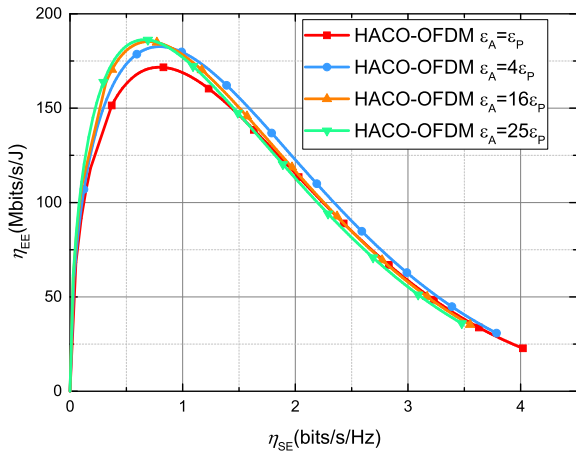
FIGURE 5. Spectral efficiency versus energy efficiency for HACO-OFDM.

The simulations are also carried out for ADO-OFDM, where the parameter μ is set to 2. The results are plotted on Fig. 6. For the low spectral efficiency, the more power ACO-OFDM possesses, the higher energy efficiency ADO-OFDM can attain. As for the largest achievable η_{SE}, $\varepsilon_A = 4\varepsilon_P$ is shown to be the optimal choice. On the one hand, if the ACO-OFDM occupies too much power, the spectral efficiency gain that DCO-OFDM produces is slight. On the other hand, DCO-OFDM suffers from the clipping noise, which means that more power allocated to DCO-OFDM can degrade the largest spectral efficiency.
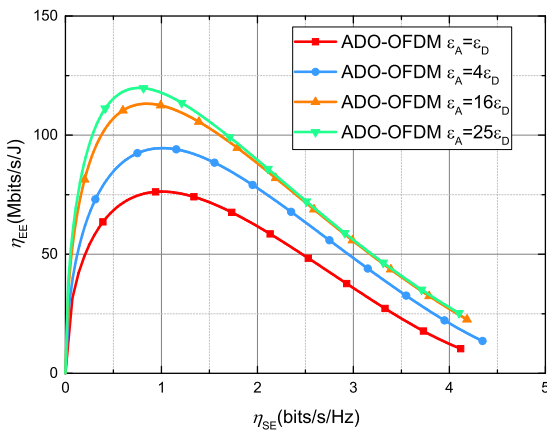

FIGURE 6. Spectral efficiency versus energy efficiency for ADO-OFDM.

Fig. 7 compares the differences of $\eta_{EE} - \eta_{SE}$ relationships with various layer numbers for LACO-OFDM. The optimal layer number, which achieves the highest energy efficiency, rises with the increase of spectral efficiency. For η_{SE} that is lower than 1 bits/s/Hz, $L = 1$ is shown to be the optimal choice, while 2-Layer LACO-OFDM outperforms the other schemes with the spectral efficiency ranging from 1 bits/s/Hz to 1.8 bits/s/Hz. For η_{SE} that is higher than 2.5 bits/s/Hz, the simulation results for 4-Layer LACO-OFDM and 5-Layer LACO-OFDM are quite close, which means the increase of the layer number can hardly bring any gain. In the perspective of the largest achievable spectral efficiency, the
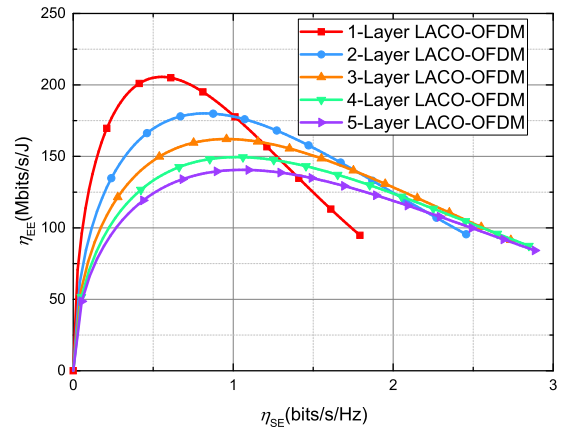

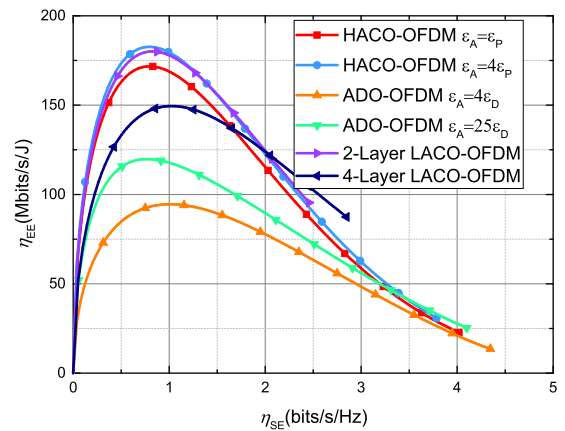**FIGURE 7.** Spectral efficiency versus energy efficiency for LACO-OFDM.

FIGURE 8. Spectral efficiency versus energy efficiency for ACO-OFDM for HACO-OFDM, ADO-OFDM, and LACO-OFDM.

LACO-OFDM with more layers has superior performance. Nevertheless, the 4-Layer and 5-Layer cases have almost the same highest η_{SE}, which is approximately 2.8 bits/s/Hz. Therefore, the optimal layer number should be adaptively chosen according to the requirement of the spectral efficiency.

Fig. 8 displays η_{EE} versus η_{SE} results for the hybrid modulation schemes, including HACO-OFDM, ADO-OFDM, and LACO-OFDM. For each scheme, two curves are selected based on the results in Figs. 5-7. As the graph shows, HACO-OFDM and 2-Layer LACO-OFDM have the superior performances for a relative low spectral efficiency. For $2 < \eta_{SE} < 3$, 4-Layer LACO-OFDM is the most energy efficient scheme. Despite of relatively low energy efficiency, ADO-OFDM can achieve a wider spectral efficient range compared with the other hybrid methods. Therefore, the optimal modulation schemes should be adaptively selected based on the application requirement.

V. CONCLUSIONS
The energy efficiency and spectral efficiency for the conventional and hybrid OFDM-based VLC modulation schemes are formulated in this paper, which assists in ensuring the QoS with affordable energy. The parameters such as the DC

Y. Sun *et al.*: Overview of OFDM-Based VLC Systems From the Perspective of Energy Efficiency Versus Spectral Efficiency

IEEE*Access*

bias in DCO-OFDM, the power allocation in HACO-OFDM and ADO-OFDM, the layer number in LACO-OFDM have various effects on the energy efficiency and spectral efficiency. The comparisons of these schemes are explored by theoretical analysis and computer simulations. Different schemes have varied performances in terms of energy efficiency whereas the achievable ranges of spectral efficiency are diverse. For practical application, the optimal scheme should be adaptively chosen with comprehensive consideration of the requirements of transmission and illumination as well as the tradeoff between energy and spectral efficiency.

REFERENCES

[1] S. Dimitrov and H. Haas, ''Information rate of OFDM-based optical wireless communication systems with nonlinear distortion,'' *J. Lightw. Technol.*, vol. 31, no. 6, pp. 918–929, Mar. 15, 2013.

[2] A. Jovicic, J. Li, and T. Richardson, ''Visible light communication: Opportunities, challenges and the path to market,'' *IEEE Commun. Mag.*, vol. 51, no. 12, pp. 26–32, Dec. 2013.

[3] M. Z. Chowdhury, M. T. Hossan, A. Islam, and Y. M. Jang, ''A comparative survey of optical wireless technologies: Architectures and applications,'' *IEEE Access*, vol. 6, pp. 9819–9840, Jan. 2018.

[4] J. Armstrong, ''OFDM for optical communications,'' *J. Lightw. Technol.*, vol. 27, no. 3, pp. 189–204, Feb. 1, 2009.

[5] J. Gancarz, H. Elgala, and T. D. C. Little, ''Impact of lighting requirements on VLC systems,'' *IEEE Commun. Mag.*, vol. 51, no. 12, pp. 34–41, Dec. 2013.

[6] J. Armstrong and A. J. Lowery, ''Power efficient optical OFDM,'' *Electron. Lett.*, vol. 42, no. 6, pp. 370–372, Mar. 2006.

[7] S. C. J. Lee, S. Randel, F. Breyer, and A. M. J. Koonen, ''PAM-DMT for intensity-modulated and direct-detection optical communication systems,'' *IEEE Photon. Technol. Lett.*, vol. 21, no. 23, pp. 1749–1751, Dec. 1, 2009.

[8] J. B. Carruthers and J. M. Kahn, ''Multiple-subcarrier modulation for nondirected wireless infrared communication,'' *IEEE J. Sel. Areas Commun.*, vol. 14, no. 3, pp. 538–546, Apr. 1996.

[9] S. D. Dissanayake, K. Panta, and J. Armstrong, ''A novel technique to simultaneously transmit ACO-OFDM and DCO-OFDM in IM/DD systems,'' in *Proc. IEEE GLOBECOM Workshops*, Dec. 2011, pp. 782–786.

[10] B. Ranjha and M. Kavehrad, ''Hybrid asymmetrically clipped OFDM-based IM/DD optical wireless system,'' *IEEE/OSA J. Opt. Commun. Netw.*, vol. 6, no. 4, pp. 387–396, Apr. 2014.

[11] Q. Wang, C. Qian, X. Guo, Z. Wang, D. G. Cunningham, and I. H. White, ''Layered ACO-OFDM for intensity-modulated direct-detection optical wireless transmission,'' *Opt. Express*, vol. 23, no. 9, pp. 12382–12393, May 2015.

[12] A. J. Lowery, ''Enhanced asymmetrically clipped optical ODFM for high spectral efficiency and sensitivity,'' in *Proc. Opt. Fiber Commun. Conf. Exhibit. (OFC)*, Mar. 2016, pp. 1–3.

[13] M. S. Islim, D. Tsonev, and H. Haas, ''On the superposition modulation for OFDM-based optical wireless communication,'' in *Proc. IEEE Global Conf. Signal Inf. Process. (GlobalSIP)*, Orlando, FL, USA, Dec. 2015, pp. 1022–1026.

[14] L. Deng, Y. Rui, P. Cheng, J. Zhang, Q. T. Zhang, and M. Li, ''A unified energy efficiency and spectral efficiency tradeoff metric in wireless networks,'' *IEEE Commun. Lett.*, vol. 17, no. 1, pp. 55–58, Jan. 2013.

[15] C. Xiong, G. Y. Li, S. Zhang, Y. Chen, and S. Xu, ''Energy- and spectral-efficiency tradeoff in downlink OFDMA networks,'' *IEEE Trans. Wireless Commun.*, vol. 10, no. 11, pp. 3874–3886, Nov. 2011.

[16] O. Amin, E. Bedeer, M. H. Ahmed, and O. A. Dobre, ''Energy efficiency-spectral efficiency tradeoff: A multiobjective optimization approach,'' *IEEE Trans. Veh. Technol.*, vol. 65, no. 4, pp. 1975–1981, Apr. 2016.

[17] E. Li, W. Zhang, J. Sun, C.-X. Wang, and X. Ge, ''Energy-spectral efficiency tradeoff of visible light communication systems,'' in *Proc. IEEE/CIC Int. Conf. Commun. China (ICCC)*, Jul. 2016, pp. 1–5.

[18] I. S. Gradshteyn and I. M. Ryzhik, *Table of Integrals, Series, and Products*. New York, NY, USA: Academic, 2014.

[19] S. D. Dissanayake and J. Armstrong, ''Comparison of ACO-OFDM, DCO-OFDM and ADO-OFDM in IM/DD systems,'' *J. Lightw. Technol.*, vol. 31, no. 7, pp. 1063–1072, Apr. 1, 2013.

[20] J. M. Kahn and J. R. Barry, ''Wireless infrared communications,'' *Proc. IEEE*, vol. 85, no. 2, pp. 265–298, Feb. 1997.

[21] K. Lee, H. Park, and J. R. Barry, ''Indoor channel characteristics for visible light communications,'' *IEEE Commun. Lett.*, vol. 15, no. 2, pp. 217–219, Feb. 2011.

[22] D. A. Basnayaka and H. Haas, ''Hybrid RF and VLC systems: Improving user data rate performance of VLC systems,'' in *Proc. IEEE 81st Veh. Technol. Conf. (VTC Spring)*, May 2015, pp. 1–5.

[23] K. Cai, M. Jiang, and X. Ma, ''Photodetector selection aided multiuser MIMO optical OFDM imaging visible light communication system,'' *IEEE Access*, vol. 4, pp. 9870–9879, Dec. 2016.

[24] R. Mesleh, H. Elgala, and H. Haas, ''LED nonlinearity mitigation techniques in optical wireless OFDM communication systems,'' *IEEE/OSA J. Opt. Commun. Netw.*, vol. 4, no. 11, pp. 865–875, Nov. 2012.

[25] X. Ling, J. Wang, X. Liang, Z. Ding, and C. Zhao, ''Offset and power optimization for DCO-OFDM in visible light communication systems,'' *IEEE Trans. Signal Process.*, vol. 64, no. 2, pp. 349–363, Jan. 2016.

[26] Y. Sun, F. Yang, and J. Gao, ''Comparison of hybrid optical modulation schemes for visible light communication,'' *IEEE Photon. J.*, vol. 9, no. 3, Jun. 2017, Art. no. 7904213.

YAQI SUN received the B.Eng. degree from the Department of Electronic Engineering, Tsinghua University, Beijing, China, in 2017, where she is currently pursuing the M.Eng. degree with the Department of Electronic Engineering. Her research interests include visible light communication and modulation.

FANG YANG (M'11–SM'13) received the B.S.E. and Ph.D. degrees in electronic engineering from Tsinghua University, Beijing, China, in 2005 and 2009, respectively. He is currently an Associate Professor with the Research Institute of Information Technology, Tsinghua University. He has published over 120 peer-reviewed journal and conference papers. He holds over 40 Chinese patents and 2 PCT patents. His research interests lie in the fields of channel coding, channel estimation, interference cancellation, and signal processing techniques for communication system, especially in power line communication, visible light communication, and digital television terrestrial broadcasting. He received the IEEE Scott Helt Memorial Award (best paper award in the IEEE TRANSACTIONS ON BROADCASTING) in 2015. He is the Secretary General of Sub-Committee 25 of the China National Information Technology Standardization (SAC/TC28/SC25). He currently serves as an Associate Editor for the IEEE ACCESS.

LING CHENG (M'10–SM'15) received the B.Eng. degree *(cum laude)* in electronics and information from the Huazhong University of Science and Technology in 1995, and the M.Ing. degree *(cum laude)* in electrical and electronics engineering and the D.Ing. degree in electrical and electronics engineering from the University of Johannesburg in 2005 and 2011, respectively. In 2010, he joined the University of the Witwatersrand, where he was promoted to an Associate Professor in 2015. He has been serving as the Secretary of the IEEE South African Information Theory Chapter since 2012. He has been a visiting professor at four universities and the principal advisor for over 30 full research post-graduate students. His research interests are in digital communications and information theory. He has published more than 70 research papers in journals and conference proceedings. He was a recipient of the Chancellor's Medal in 2005 and the National Research Foundation rating in 2014. The IEEE ISPLC 2015 Best Student Paper Award was made to his Ph.D. student in Austin.

• • •